Doppler-Free Spectroscopy

MIT Department of Physics

Traditionally, optical spectroscopy had been performed by dispersing the light emitted by excited matter, or by dispersing the light transmitted by an absorber. Alternatively, if one has available a tunable monochromatic source (such as certain lasers), a spectrum can be measured one wavelength at a time' by measuring light intensity (fluorescence or transmission) as a function of the wavelength of the tunable source. In either case, physically important structures in such spectra are often obscured by the Doppler broadening of spectral lines that comes from the thermal motion of atoms in the matter. In this experiment you will make use of an elegant technique known as Doppler-free saturated absorption spectroscopy that circumvents the problem of Doppler broadening. This experiment acquaints the student with saturated absorption laser spectroscopy, a common application of **non-linear optics**. You will use a diode laser system to measure hyperfine splittings in the $5^2S_{1/2}$ and $5^2P_{3/2}$ states of ^{85}Rb and ^{87}Rb.

I. PREPARATORY PROBLEMS

1. Suppose you are interested in small variations in wavelength, $\Delta\lambda$, about some wavelength, λ. What is the expression for the associated small variations in frequency, $\Delta\nu$? Now, assuming $\lambda = 780nm$ (as is the case in this experiment), what is the conversion factor between wavelength differences ($\Delta\lambda$) and frequency differences($\Delta\nu$), in units of GHz/nm?

2. Suppose you have a laser cavity of length, L, and with index n. What are the frequency and wavelength spacings $\Delta\nu$ and $\Delta\lambda$ of the longitudinal cavity modes for radiation at wavelength λ? Compute the value of $\Delta\nu$ and $\Delta\lambda$ for (a) a diode laser with: $\lambda = 780$ nm, $L = 250$ μm, $n = 3.5$ and (b) a 2 cm external cavity diode laser with: $\lambda = 780$ nm, $L = 2$ cm, $n = 1$.

3. Draw an energy level diagram for ^{85}Rb and ^{87}Rb including the ground state (5S) and first excited state (5P) showing the fine structure (spin-orbit coupling) and hyperfine structure (nuclear angular momentum). Include estimates of the energy scales for the different interactions.

4. Make a chart or diagram of as many different frequency (e.g. energy, wavelength, etc.) scales in this experiment as you can using approximate values and units of MHz: Laser linewidth, laser longitudinal mode spacing, natural atomic linewidth, fine structure, hyperfine structure, Doppler width, Fabry-Perot free spectral range, Fabry-Perot resolution, wavemeter resolution, ...

5. Explain how a diode laser works, including what elements constitute the resonant optical cavity, the gain medium and the source of pump energy.

II. LASER SAFETY

You will be using a medium low power ($\approx$ 40 mW) near-infrared laser in this experiment. The only real damage it can do is to your eyes. Infrared lasers are especially problematic because the beam is invisible. You would be surprised how frequently people discover they have a stray beam or two shooting across the room. Additionally, laser work is often done in the dark, which causes the pupil of the eye to dilate, making you that much more vulnerable.

ALWAYS USE THE APPROPRIATE LASER SAFETY GOGGLES WHEN THE LASER IS ON.

Keep the doors closed and windows covered, to protect people outside the room. To the industrious student, we leave the following theoretical exercise: compare the power per unit area hitting your retina if where you to look directly at the sun with that if you where you to look directly into a 10 mW laser beam of 1 mm diameter (but don't actually try it!).

CAUTION: FRYING THE DIODE LASER

The diode laser is an extremely delicate electronic device. It can very easily be destroyed or damaged by static electricity or by subjecting it to relatively small currents. The maximum current is limited by the sophisticated laser controller you will be using, but generally you should stay around a setting of 55 mA. Additionally, there are omnipresent current spikes from static electricity and the switching on and off of nearby electrical equipment, including the laser power supply itself. Such current spikes are regularly implicated in the frequent and untimely deaths of diode lasers. Diode lasers cost money, they can be hard to obtain, and it is definitely not any fun to install a new one and realign the laser diode head. So help us out by following theses rules:

DO NOT DISCONNECT THE LASER HEAD FROM THE CONTROLLER OR ATTEMPT TO DRIVE THE LASER WITH A DIFFERENT POWER SUPPLY.

CAUTION: CARE OF THE OPTICS

You will be using expensive precision optical instru-

ments, so treat the equipment with great care. Even a good front-surface mirror can cost quite a bit.

ALL OPTICAL SURFACES (INCLUDING MIRRORS) SHOULD ONLY BE CLEANED WITH COMPRESSED AIR OR DELICATELY SWABBED WITH LENS TISSUE MOISTENED WITH LENS CLEANER. NEVER SCRUB.

III. INTRODUCTION

There are many varied references which may prove useful in performing this lab. They are listed in the bibliography [1–13].

Saturated absorption laser spectroscopy requires a quasi-monochromatic, tunable, highly directional, laser beam to excite atoms from lower levels, $|g\rangle$, to excited levels, $|e\rangle$. For stationary atoms, absorption from the laser beam is maximum when the laser frequency ν_L exactly coincides with an atomic transition ν_0. The resonance is sharp in this case, meaning that absorption is confined to a very narrow range of frequencies. This situation changes, however, when the atoms are moving. Consider an atom *moving* toward the laser with a velocity v along the beam. If this atom is to experience maximum absorption, ν_L must now be reduced because of the Doppler effect: an atom moving toward a source of light "observes" the light to be upshifted in frequency due to the relative motion. Hence, a reduction in ν_L is mandatory if, after this upshifting, the frequency of the light in the atom's frame is to match the transition frequency ν_0 . The magnitude of the required shift is $\delta\nu \cong \nu_0\left(\frac{v}{c}\right)$, which calls for a downshift or upshift in the laser frequency depending on whether the atom is approaching ($v < 0$) or receding ($v > 0$) from the laser.

Consider a gaseous sample of atoms through which a laser beam passes. The number of atoms $N(v)dv$ lying within some velocity interval dv, when plotted as a function of velocity v along the beam, yields a bell-shaped "Maxwellian" distribution centered at $v = 0$. Since a majority of the atoms exhibit only modest velocities, most of these velocities will fall near the middle of the distribution. The remaining atoms, with larger velocities along the beam, populate the wings of the distribution. One can show that a majority of the atoms in the sample have velocity components v on the order of $\sqrt{\frac{2kT}{M}}$, where M is the mass of the atom, k is Boltzmann's constant, and T the absolute temperature. It follows that a gaseous target exhibits a range of absorption frequencies due to this spread in velocities and associated Doppler shifts. The width [FWHM] of this inhomogeneously-broadened Doppler spectral profile is

$$\Delta\nu_D = 7.16\ \nu_0\sqrt{\frac{T}{A}} \times 10^{-7} \qquad (1)$$

where A is the atomic weight. According to this expression, a sample of rubidium atoms, maintained at 297 K and excited at 780 nm ($\nu_0 = 3.8\times10^{14}$ Hz), will exhibit a Doppler width of 502 MHz. This is one prediction that is to be tested in the present experiment.

For many years, Doppler widths on the order of 500 MHz served to limit the resolution of optical spectroscopy. Various atomic and molecular interactions, presumed to be small but capable of producing significant features in optical spectra, were never observed because of shrouding and broadening due to the Doppler effect.

The primary feature of saturated absorption laser spectroscopy is its avoidance of or insensitivity to the Doppler effect.

Hence spectra produced by this technique are referred to as "Doppler-free." As such, they exhibit much greater sharpness/resolution, and they reveal spectroscopic features that were heretofore unobservable.

The term "velocity group" is important in saturated absorption laser spectroscopy. It is an abbreviation for a group of $N(v)dv$ atoms, all of which have velocities between v and $v + dv$ along the laser beam. Velocity groups exhibit different sizes - groups near the center of the distribution are large while groups located in the wings of the distribution are small. The term "population" is also important; it is short for the number of atoms or atomic population that occupies a specific atomic state $|n\rangle$. Ground-state populations are much larger than excited-state populations although saturated absorption laser spectroscopy is capable of producing significant redistributions within these populations. The dots in Fig. 1a depict relative populations; in the case shown here, the ground-to-excited-state population ratio is 5:2. The bell-shaped curves in Fig. 1b go a step further by depicting the Maxwellian velocity distributions $N_g(v)dv$ and $N_e(v)dv$ for the ground and excited-state populations.

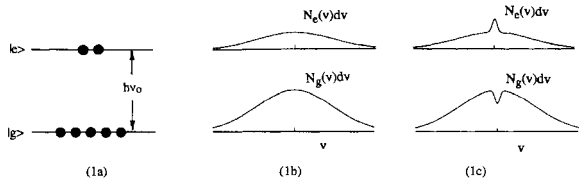

FIG. 1. Population and Maxwellian velocity distributions in a ground-state, $|g\rangle$, and and excited-state, $|e\rangle$, for a hypothetical two-state atom. The hole-burning and population redistribution shown in part (c) correspond to a laser frequency $\nu = \nu_0$.

Consider next the case of a laser beam with frequency $\nu = \nu_0$. Fig. 1c indicates what happens when such a beam passes through a gaseous sample. Only the $v = 0$ group in the ground state interacts with this beam, and hence this group is the only one that suffers depopulation due to promotion of atoms into the excited state.

One says that the laser has burned a "hole" in the middle of the ground-state distribution since fewer $v = 0$

atoms remain to absorb laser light. Such hole-burning or depopulation is central to saturated absorption laser spectroscopy. In the two-level case considered here, this phenomenon requires considerable laser power and/or a relatively long excited-state lifetime τ. The long lifetime helps because it delays the atom's return to the original state. The probability for such decay per unit time is $\Gamma = \frac{1}{\tau}$. Since τ is 28 nsec for the $5^2P_{3/2}$ state of Rb, the spontaneous decay rate here is $\Gamma = 0.36 \times 10^8$ sec^{-1}.

Suppose that the laser frequency ν exceeds the resonant frequency ν_0. It follows that ground-state atoms in the $v = 0$ velocity group can no longer absorb. The only group that can absorb is the group that is moving away from the laser with the right velocity $v > 0$ so as to see the laser frequency ν downshifted to the correct resonant frequency ν_0. Due to the absorption, a hole or relative shortage of atoms develops in this particular $v > 0$ group. We see that as the laser frequency ν continues to scan through the resonance, this hole shifts from group to group.

Saturated absorption laser spectroscopy employs two laser beams derived from a single laser to insure that they both have the same frequency. The beams are arranged to propagate in opposite directions and overlap one another as they pass through the target. One beam, the "pump" beam, is more intense. The other, usually 1/10 as intense, is called the "probe" beam.

Consider the effects of two such beams on a gaseous sample as the laser frequency ν scans upward toward ν_0. For a specific $\nu < \nu_0$, the group of atoms that interacts with the pump beam is that group which counterpropagates along this beam with the requisite velocity $v < 0$ that tunes the beam and atoms into resonance. The only other group of affected atoms is the group that counterpropagates with the same speed relative to the probe beam. These two velocity groups lie in opposite wings of the ground-state distribution. The pump beam burns a significant hole in its $v < 0$ group, but the probe beam, because of its low intensity, causes negligible redistribution within its group.

To perform saturation spectroscopy, one monitors the amount of absorption that the probe beam undergoes as it passes through the sample. If $P(\nu)$ represents the power carried by the probe beam after passage through the sample, one can define an absorption signal $A(\nu) = P_b - P(\nu)$ where $P(\nu)$ is assumed to approach a constant or "baseline" level of transmitted power P_b far from the resonance. We assume P_b to be frequency independent and note that $A(\nu)$ provides a direct measure of the frequency-dependent absorption by the sample. As the laser frequency ν continues to approach ν_0, the sample's absorption $A(\nu)$ from the probe beam gradually increases due to the increasing population of the velocity groups.

If the pump beam happens to be blocked while the laser scans right through ν_0, the absorption signal $A(\nu)$ associated with the probe beam shows a simple, Doppler-broadened lineshape that reflects the varying sizes of the velocity groups in the ground-state distribution.

Now we return to the two-beam case, and let the laser $\nu = \nu_0$. Now the pump and probe beams interact with the same group of atoms, the $v = 0$ group. The pump beam proceeds to depopulate this group, and the probe finds as a result that there are fewer $v = 0$ atoms than in nearby groups. It follows that the absorption of energy $A(\nu)$ from the probe beam exhibits a sharp dip at ν_0 due to this depopulation by the pump. According to the probe, the sample's absorption capacity at $\nu = \nu_0$ shows fatigue or "saturation," and $A(\nu)$ no longer reflects just the gradual variation in $N_g(v)dv$. Instead, the lineshape $A(\nu)$ exhibits the sharp dip called a Lamb dip characteristic of "saturated absorption." A Lamb dip can be several orders of magnitude narrower than the Doppler-broadened spectrum on which it sits. Therein lies the reason why saturated absorption signals can resolve previously shrouded features and offer the prospect of increased spectroscopic accuracy and precision.

The width of the Lamb dip is finite, however, for several reasons, the most fundamental being the uncertainty principle. In the limiting case for which (1) the laser beams are monochromatic and weak, (2) atomic collisions are rare, and (3) the atomic dwell time in the laser beam is long, the width of the Lamb dip is $\delta\nu = \frac{\Gamma}{2\pi}$ which is the "natural width" of the transition. In the present case of Rb, $\delta\nu = 6$ MHz [FWHM]. Lamb dips this narrow are not achieved in the current experiment because our free-running diode laser is insufficiently monochromatic. Since the spectral width of the laser used here is about 30 MHz, the widths of our Lamb dips are 30-40 MHz.

III.1. Fine and Hyperfine Structure

As an alkali metal with one valence electron, Rb has an energy-level scheme that resembles hydrogen. The ground state is designated $5^2S_{1/2}$ and the first excited states, the $5^2P_{1/2}$ and $5^2P_{3/2}$, derive their splitting (their fine-structure splitting) from the spin-orbit interaction. This representation of the electron configuration in multi-electron atoms is called Russell-Saunders notation. The term symbol provides information about the angular momentum quantum numbers in the given energy state. The term symbol takes the form $^{2S+1}L_J$, where S is the total spin quantum number, J is the total orbital angular momentum quantum number, and L is the orbital quantum number in spectroscopic notation (S,P,D,...). Additionally $2S + 1$ is the spin multiplicity: the maximum number of different states for a given J. The notation preassumes spin-orbit coupling in the atom. This experiment involves the $5^2P_{3/2}$ state, which lies an energy equivalent of 780 nm above the $5^2S_{1/2}$ ground state.

If the rubidium nuclei were spinless, the $5^2S_{1/2}$ and $5^2P_{3/2}$ energy levels would be singlets in the absence of external fields. Such is not the case, however; natural rubidium contains two isotopes, the 28% abundant ^{87}Rb (I=3/2) and the 72% abundant ^{85}Rb (I=5/2). These non-zero nuclear spins dictate that rubidium nuclei ex-

hibit magnetic and possibly quadrupolar moments (in addition to charge and mass). Nuclear moments interact with the atomic electrons to generate structural subtleties called hyperfine structure (hfs) and hyperfine energy splittings.

To characterize the hfs, it is useful to define a total angular momentum quantum number F, which, in the case of the $5^2S_{1/2}$ state of ^{87}Rb, assumes the values 1 and 2. In the $5^2P_{3/2}$ state of ^{87}Rb, F can be 0, 1, 2, or 3. A transition between some hyperfine sublevel in the $5^2S_{1/2}$ state and a hyperfine sublevel in the $5^2P_{3/2}$ manifold must satisfy the selection rule $\Delta F = \pm 1$ or 0. The energies, or more precisely, the frequencies ν_F of the various hyperfine sublevels within a given $^{2S+1}L_J$ manifold such as the $5^2P_{3/2}$ can be expressed in terms of two hyperfine coupling constants A and B:

$$\nu_F = \nu_J + \frac{AC}{2} + \frac{B\left[\frac{3C(C+1)}{4} - I(I+1)J(J+1)\right]}{2I(2I-1)J(2J-1)} \quad (2)$$

where $C = F(F+1) - J(J+1) - I(I+1)$. For the $5^2S_{1/2}$ ground state of ^{87}Rb, C assumes the values -5/2 or +3/2 corresponding to $F = 1$ or 2. It follows that the third term in Eq. 2 is zero, and thus the hfs in the ground state of ^{87}Rb is characterized by the single coupling constant A($5^2S_{1/2}$). The same is true for the ground state of ^{85}Rb. As for the $5^2P_{3/2}$ state of ^{87}Rb, C varies from -15/2 to +9/2 as F ranges from 0 to 3. In this case, both coupling constants A and B are nonzero. By subtracting Eq. 2 from itself for adjacent pairs of hfs sublevels in the $5^2P_{3/2}$ manifold, one can derive three linear equations which relate three experimentally-determined hfs splittings $\Delta\nu = \nu_F - \nu_{F-1} = \alpha, \beta$ and γ to a single pair of coupling constants A and B. **The determination of such a pair (A, B) is the major objective of this experiment**.

IV. APPARATUS

All lasers rely of several common principles for operation: most notably stimulated emission of radiation and population inversion. According to quantum mechanics, all atoms and molecules have discreet energy states which correspond to different periodic motions of the constituent nuclei and electrons. The lowest possible energy states are called the ground state of the particle while all other states are referred to as excited states. In certain circumstances, an atom or molecule can change its energy level by absorption or emission of a photon in what is called an optically allowed transition according to the resonance condition $\Delta E = h\nu$, where ΔE is the difference between initial and final energy states, h is Planck's constant and ν is the photon frequency.

There are two different emission processes, spontaneous emission and stimulated emission. Spontaneous emission is what occurs when an atom or molecule undergoes a transition from an excited energy level to a lower energy level by emitting a resonance photon, conserving total energy. In stimulated emission, a photon of energy hν perturbs the excited particle and causes it to relax to a lower level, emitting a photon of the same frequency, phase, and polarization as the perturbing photon. Stimulated emission is the basis for photon amplification and the fundamental mechanism underlying all laser action. A simplified look at laser action is now described. Einstein defined two coefficients A and B which are parameters related to a particular transition of a given material. The coefficient A relates to the spontaneous emission probability while B relates to the absorption and stimulated emission probabilities (both are equal in terms of quantum mechanical rules).

Given a very simple two level system with lower level 1 and upper level 2, the relative transition rates can be expressed in terms of N_1 and N_2 which represent the relative populations of the respective levels and the Einstein coefficients A_{21} and B_{12} (=B_{21}). The subscripts denote the direction of the transition. Under normal conditions, $N_1 >> N_2$ as predicted by statistical thermodynamics. When a resonant photon passes through a volume of these particles, it may interact with a level 1 particle and be destroyed in an absorption process, the probability of which is proportional to $N_1 \times B_{12}$. Alternatively, it may interact with an excited level 2 particle and generate a second photon of identical nature through stimulated emission with a probability proportional to $N_2 \times B_{21}$. In order for laser action to occur, a population inversion is necessary, defined by $N_2 > N_1$. Spontaneous emission also competes to deplete the N_2 level yet only produces unwanted photons of an indiscriminate character. Because of this and other losses, every laser has a minimum value of $N_2 - N_1$ which can give rise to laser output, called threshold inversion.

In order to sustain laser emission, it is necessary to enclose the excited material within an optical cavity (i.e. between two reflecting surfaces). In this case, photons are reflected many times through the lasing medium, greatly increasing the probability of interacting and producing stimulated emission. This multipass nature of the optical cavity results in interference-induced longitudinal mode structure. Only laser light whose wavelength satisfies the standing wave condition, $ml = 2nL$, will be amplified. L is the cavity length, n is the refractive index of the material, and m is an integer corresponding to the mode number of the standing wave pattern. The spacing of adjacent modes is given by $\Delta\nu = \frac{c}{2nL}$, where c is the speed of light. For $n = 6$, $L = 250$ μm then the spacing is about 3.3cm^{-1} or 100 GHz. In addition to longitudinal mode structure, the radiation field may have nodes and antinodes in the plane perpendicular to the laser axis. The best mode structures follow a gaussian distribution, have minimal diffraction losses and can therefore be focused to the smallest size spot.

Broad tuning characteristics of the diode laser are controlled by the shift of the band gap with diode temperature, roughly 2 to 5 cm^{-1} K^{-1}. In our experiment the

operating temperature typically ranges between 293-323 K, which is achieved by controlling the temperature of the cold plate mount to which the diode laser package is mounted. Single mode tuning is obtained by changing the laser current. Small changes in laser current cause small changes in the crystal's temperature and thus causes a change in the refractive index n, of the semiconductor material. This refractive index (in the range of 5.5 to 6.5 for Pb-salt materials) change causes a frequency shift according to the relation

$$\Delta\left(\frac{1}{\lambda}\right) = \frac{1}{2L(n - \lambda\frac{\partial n}{\partial \lambda})} \tag{3}$$

where L is the length of the laser cavity (the change of L with temperature is negligible). Note that a combination of different operating temperatures and currents will provide a selection of different frequencies of emitted radiation. Diode lasers tend to emit energy in fewer modes at lower current levels (relative to threshold) and single mode operation generally occurs at higher operating temperatures. Thus it is desirable to access absorption features using combinations of low current and high temperatures. The tuning rate of the laser is determined by the thermal resistance of the device as well as by the electrical contact resistance (.005 to .05 ohm) which is much greater than the bulk resistance of the material. Typical rates are between .001 to .017 cm^{-1} mA^{-1} (250 MHz mA^{-1}). Since the thermal resistance of the diode laser package increases with temperature, tuning rates are typically larger at higher operating temperatures.

Radiation emitted from diode lasers consists of energy which is highly divergent as well as being quite astigmatic. Half-angle divergence in the direction perpendicular to the active or junction layer is typically between 12 and 30 degrees (with 90 degrees occurring as well) while the radiation divergence in the plane parallel to this layer is typically 2 to 6 times less.

You will be using a commercial external cavity diode laser system manufactured by TUI Optics, in this experiment. This unit consists of a laser head and a controller. The head contains the 780nm AlGaAs semiconductor diode laser together with a collimating lens, mounted on a temperature controlled stage. The design incorporates a diffraction grating placed in front of the diode, which acts as a wavelength selective mirror; since this mirror forms one of the two reflective surfaces of the laser cavity its orientation thus allows fine tuning of the output frequency of the laser. Such an *external cavity diode laser* can output single mode light with a spectral width of 30 MHz or less. Changing the diode current and the diode temperature can also change the output frequency, but more drastically (often causing mode hopping, and also changing the output power).

The controller (Fig. 2) is turned on by rotating the key clockwise; be sure to turn it off after you are done. It consists of four modules: the main DC100 monitor, the DTC100 temperature controller, the DCC100 current controller, and the SC100 scan controller. The DC100 shows the diode's current and temperature. The DTC and DCC have fine adjustment knobs to set the temperature and current, and incorporate feedback loops with limit settings to allow these parameters to settle gracefully. Note that the diode temperature may take several minutes to settle down when you first turn on the system, or change the temperature. Do not modify any settings other than the large multi-turn potentiometers. The SC100 allows the diode's output frequency to be swept in a ramp; the three knobs of interest control the width of the sweep (the red knob), the sweep speed (small grey knob left of the multiturn potentiometer), and the sweep offset (the multiturn pot). A frequency sweep of approximately 10 GHz is possible, with periods from seconds to milliseconds. The SC100 has two outputs; one goes to the diode laser, and the other (the trigger) is a TTL (0/+5V) level signal used to trigger acquisition by the oscilloscope. The SC100 can be turned off when no frequency sweep is desired.

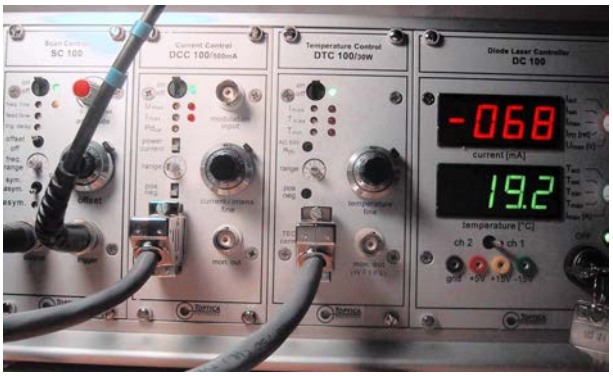

FIG. 2. Front panel of the TUI Laser.

The laser's manual, and further references on diode lasers in general, are available on the Junior Lab web site (go to the page for this lab).

IV.1. Balanced detector

The other piece of equipment special to this experiment is a balanced optical detector, used to sense the intensity *difference* of two optical beams. This is used to remove an undesirable sloping baseline in the absorption spectra which can result from scanning the laser frequency; it also allows Doppler-broadened components to be removed from the spectra, and suppresses common-mode signals that arise from stray light.

The detector is comprised of two reversed-biased PIN photodiodes wired with opposite polarities to the summing point of a current-to-voltage converter. By this means we monitor only the difference $A_{12}(\nu) = A_1(\nu) - A_2(\nu)$ between the absorption signals riding on the separate probe beams.

These beams, the rubidium vapor cell, and the dual

detector-amplifier are carefully positioned so that in the absence of a pump beam, the differential absorption signal $A_{12}(\nu)$ is null throughout the sweep. Even with the reintroduction of the pump beam, which crosses only one probe beam, the null in $A_{12}(\nu)$ persists as long as ν differs from ν_0. At resonance, however, one gets a pure saturation signal, devoid of Doppler character and riding on a flat baseline.

IV.2. Frequency meter

A Burleigh Wavemeter Jr. optical wavelength meter is available for optional use. This uses a calibrated Michaelson interferometer to measure the wavelength of light which is coupled in through an optical fiber. The input is a fiber input coupler mounted on an optical post with a special magnetic base so that it can easily be placed and removed from in front of the laser. The input angle must be aligned carefully to couple light into the fiber; it is helpful to monitor the wavemeter's photodiode current while doing this, using the BNC connector on the back. It may take several minutes to achieve good alignment. The wavemeter is good to ± 0.2 nm or so around 780 nm.

IV.3. Optical Path

The layout for this experiment is shown in Fig. 3. Light comes out of the laser head through a sliding shutter which can be used to temporarily block the beam. The laser head should be aligned (if not already done) so that the laser beam is everywhere parallel with the breadboard surface. You should always begin a session by double checking this and noting the beam height in your notebook.

The beam passes first through a Faraday isolator to reduce laser instabilities and is then split into two legs by a simple glass slide beam splitter. The reflected beam is directed into a Fabry-Perot interferometer, used to monitor the laser's frequency during a sweep. This is comprised of two partially reflective mirrors and a silicon detector. The mirrors must be aligned such that they are plane parallel. Interferometric traces generated by this cavity show that the nonlinearity of the laser sweep is about 0.2% for sweeps of 2 GHz or less.

The main laser beam is transmitted through the glass slide beam splitter and passed through a variable neutral density filter wheel. This is used to control the overall power in the pump and probe beams and thus to minimize the power broadening of the Rb spectral lines. Following the variable neutral density filter, the beam is split again by a prism. Two weak, parallel beams are reflected from its surfaces; these are used as the probe beams. The un-reflected high-power beam is the pump. Two mirrors reflect the pump and probe beams toward each other, intersecting at the Rb cell. All three beams pass through the cell, but only one probe beam intersects the pump inside the cell. The two probe beams then go into the balanced detector. Additional neutral density filters can be placed inline with the probe and pump beams to control their levels independently.

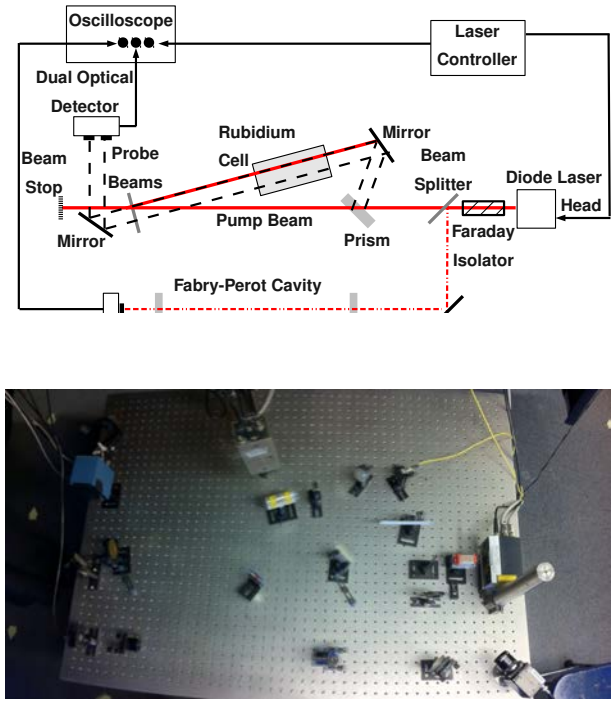

FIG. 3. Experimental Layout: (top) schematic, (bottom) actual photo of optical breadboard.

Our choice of the D_2 transition in atomic Rb is prompted by several considerations:

1. single-mode external cavity laser diode systems work well at the requisite 780 nm wavelength;
2. in a darkened room, the 780 nm light is visible and easily tracked with the help of a phosphorescent beam plate;
3. the atomic target consisting of a static Rb cell at room temperature is very convenient;
4. natural rubidium, with its $^{85}Rb(72\%)$ and $^{87}Rb(28\%)$ isotopes, invites measurement of ground and excited-state hyperfine splittings as well as Doppler widths and isotope shifts; and
5. the energy-level scheme of Rb automatically provides optical pumping, which significantly enhances the saturated absorption effect.

V. OBSERVATIONS AND MEASUREMENTS

A typical experiment will involve the following steps:

1. Align the Fabry-Perot cavity and tune the laser such that interference fringes are visible with a reasonable sweep range.

2. Align the pump and probe beams through the Rb cell and find the ^{87}Rb fine and hyperfine transitions using the diode settings you found.

3. Try different pump and probe beam attenuation levels using different neutral density filters, to observe the doppler broadened peak, the Lamb dip, and finally sharp doppler-free spectra.

4. Quantitatively measure the splittings of the peaks and the peak separations, using the Fabry-Perot interference fringes for frequency difference calibration.

5. Derive the coupling constants A and B of Eq. 2 from your measurements.

V.1. Lineshape Considerations

One of the chief difficulties of this experiment is achieving a good balance of pump and probe power to minimize the observed linewidths, and some theory can help explain what we should observe. Pappas et al. [4] have analyzed the present situation in which optical pumping significantly enhances saturated absorption effects. These authors show that in this case, the differential lineshape $A_{12}(\nu)$ for saturated absorption by a low-density target is

$$A_{12}(\nu) = A_s\Big(\frac{\Delta}{2}\Big)^2\left[(\nu-\nu_0)^2+\Big(\frac{\Delta}{2}\Big)^2\right]^{-1} \tag{4}$$

where A_s scales as

$$I_{probe}\frac{I_{pump}}{I_{sat}}\frac{1-\Gamma_i T}{2+\Gamma_i T}\left[F+F^2\right] \tag{5}$$

and $\Delta = \frac{\gamma(1+F)}{4\pi}$ is the power-broadened width [FWHM] of the signal in Hz. The quantities I_{probe} and I_{pump} are beam intensities, $F = \sqrt{1+\frac{I_{pump}}{I_{sat}}}$ is the broadening factor, $\gamma = \frac{1}{\tau}+\frac{2}{T}+2\pi\delta\nu_{laser}$ is the homogeneous linewidth of the transition in rad/sec, and $I_{sat} = \frac{h\nu_0}{\sigma_0\tau}(1+\frac{\tau}{T})(2+\Gamma_i T)^{-1}$ is a convenient yardstick by which to measure of the intensity of the pump beam. In this expression, ν_0 is the transition frequency between a hyperfine level of the $5^2S_{1/2}$ ground state and the ith hyperfine level of the excited $5^2P_{3/2}$ manifold, τ is the lifetime of the $5^2P_{3/2}$ state,Γ_i represents the sum over all spontaneous decay rates from the ith excited hyperfine level to all lower levels except the initial one, and T is the duration of the excitation (the time that the atoms remain in the laser beam).

The absorption cross section per atom is

$$\sigma_0 = \frac{16\pi^2 k\mu^2}{h\gamma}\frac{1}{4\pi\epsilon_0} \tag{6}$$

where $k = \frac{\omega}{c}$, the electric dipole moment μ satisfies

$$\mu^2 = \frac{2\epsilon_0 hc^3\Gamma_0}{2\omega_0^3} \tag{7}$$

and Γ_0 is the spontaneous decay rate peculiar to the resonant pair of hyperfine levels. The values of Γ_i and Γ_o reflect hyperfine branching ratios and satisfy the equation $\Gamma_i+\Gamma_o = \frac{1}{\tau}$. Large values for the Γ_i portend significant optical pumping, which implies enhanced saturation absorption signals. A large value of Γ_o , on the other hand, implies a strong transition moment but not necessarily a strong saturation signal.

While the previous discussion is somewhat dense, its significance is straight-forward: one can easily determine or estimate ν_0, τ, T, and $\delta\nu_{laser}$

With a little more effort, one can find values for Γ_o and Γ_i , and proceed to determine μ, σ_0, and I_{sat}. By measuring I_{pump}, one can then evaluate F and hence predict the power-broadened widths Δ of the saturated absorption signals. Hence, through these expressions, one can appreciate that greater pump intensities I_{pump} imply stronger but broader signals, and that large values of Γ_i imply small values of I_{sat} , which means that I_{pump} need not be large to produce sizeable saturated absorption signals in the presence of optical pumping. Finally, we see that if T is large compared to τ then in the limit of low laser power, the saturated absorption linewidth Δ is essentially $\delta\nu_{laser}$.

V.2. Aligning the Fabry-Perot

The chief challenge in using the Fabry-Perot cavity to monitor the laser frequency is alignment of the two cavity mirrors. First ensure that the laser beam enters into the Fabry-Perot cavity; the beam is often blocked when performing the spectroscopic measurements because light retro-reflected from the F-P cavity back into the diode laser can cause undesired instabilities.

Next, remove both mirrors and make sure the laser beam is parallel with the optical bench and falls at the center of the silicon detector. Locate the pinhole (or adjustable iris) and check that the laser goes through it. Place this in front of the front F-P mirror, then insert the back F-P mirror (the one nearest the detector). Look for the mirror's reflection on the surface of the pinhole and align the mirror until the reflection passes back through the pinhole. Now insert the front mirror and repeat. It is helpful to use the CCD camera to observe the reflection. Now turn on the SC100 frequency sweep and train the CCD on the detector.

Tweak up both mirrors until you see clear interference fringes on the detector. When properly aligned, the detector should produce an output voltage with a swing of

$\approx$ 30 mV which is easily observed on the scope. Figure 4 shows a sample of actual data from this procedure. If you do not see fringes, it may be because the laser is not operating in its single mode regime. You will want to set the SC100 on its widest sweep range, and initially zero the SC100 offset. A diode current of about 54 mA and temperature of 18.0° C are good choices to begin with. Be sure to measure the F-P mirror separation so you can calculate its free spectral range later. Experiment with the diode laser settings to determine for what ranges you get single-mode output.

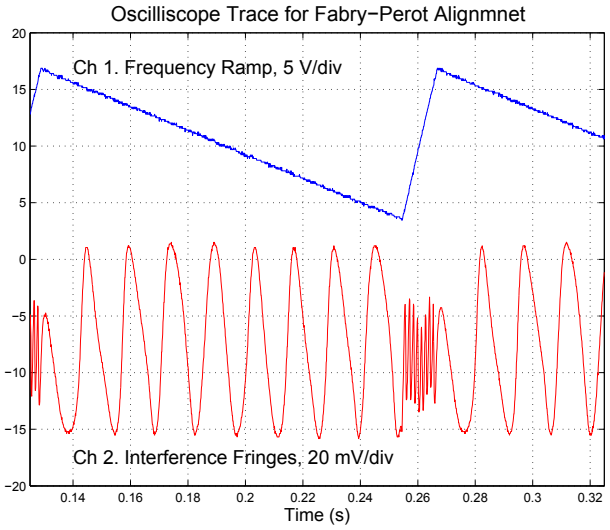

FIG. 4. Sample Data for the Oscilliscope reading of the Fabry-Perot Interferometer

V.2.1. Saturated Absorption Spectra

Figure 5 shows three types of absorption lineshapes that can be obtained from the experimental layout shown in Figure 3. To produce spectrum 1, both the pump and one of the probe beams must be blocked. Hence this spectrum, which records the absorption $A(\nu)$ of the vapor vertically versus laser frequency horizontally, is a conventional Doppler-broadened lineshape. The two large features in the center of the spectrum arise from the more abundant isotope ^{85}Rb while the outer lobes arise from ^{87}Rb. These features come in pairs because of the hyperfine interaction and hence splittings in the $5^2S_{1/2}$ ground state. The hfs splitting for ^{87}Rb, being nearly double that of ^{85}Rb, suggests that the former's nuclear magnetic moment is roughly double the latter's.

Trace 2 in Figure 5 was acquired with one pump and one probe beam. Various Lamb dips, most of which are not fully resolved, are now present. With only one probe beam, the Doppler character remains, but the trace shows unmistakably how saturated absorption appears as fatigue in the absorption capacity of the sample. Notice that in your measurements, traces on the scope may ap-

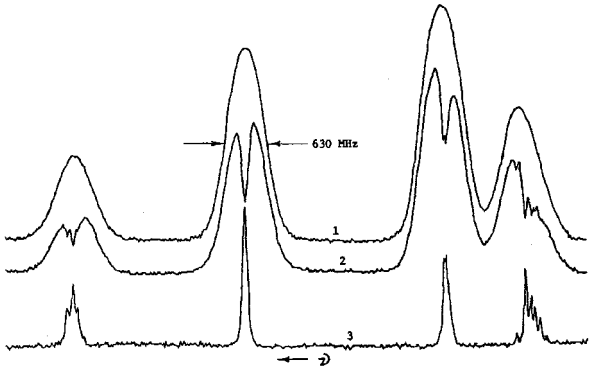

FIG. 5. Three different absorption spectra acquired with the setup of Fig. 3.

pear with different polarity and pedestals; however the difference will look like trace 3.

Finally in trace 3 we see the effects of using two probe beams. Here we have the differential signal A_{12}, and we see that saturated absorption laser spectroscopy reveals at least nine new features that were completely shrouded in trace 1. These new features arise from hfs splittings in the $5^2P_{3/2}$ state. Note from the flatness of the baseline that all the Doppler character has been removed from this spectrum.

Align the pump and probe beams such that you can see data like those of traces 1 and 2. Make sure the laser is operating in its single-mode regime. You may need to block the beam from entering the F-P cavity to prevent laser instabilities from the F-P retroreflection into the laser.

V.2.2. Balancing the detector

The pump and two probe beams, the rubidium vapor cell, and the dual detector-amplifier are carefully positioned so that in the absence of a pump beam, the differential absorption signal $A_{12}(\nu)$ is null throughout the sweep. Even with the reintroduction of the pump beam, which crosses only one probe beam, the null in $A_{12}(\nu)$ persists as long as ν differs from ν_0. At resonance, however, one gets a pure saturation signal, devoid of Doppler character and riding on a flat baseline.

Neutral density filters attenuate the laser beams to optimize the tradeoff between signal size and signal width. Since the collimated beams have areas of about $5mm^2$, the probe and pump powers of 10 and 100 μW correspond to beam intensities of 2 and 20 $\frac{\mu W}{mm^2}$ respectively. Low laser noise obviates the need for beam chopping and synchronous detection.

Place neutral density filters in both the probe and pump beam paths, and align the balanced detector until you have data such as that of trace 3. Note that the detector sits on a translating stage which can be moved if you loosen the lock-down screw. A typical differential

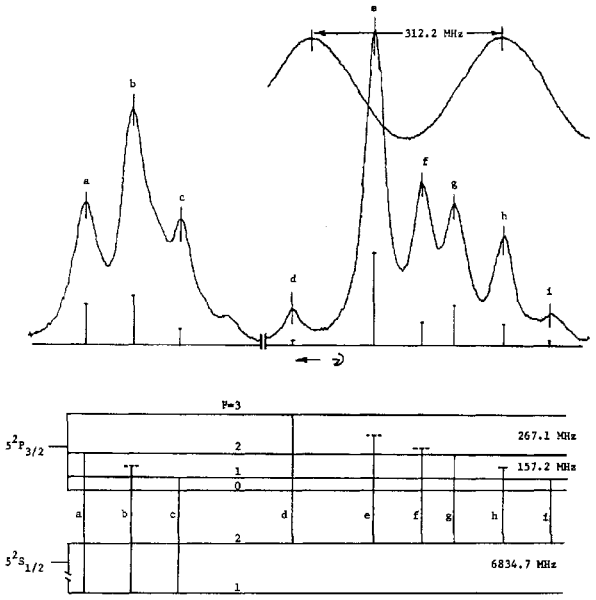

FIG. 6. Composite saturated absorption spectrum for ^{87}Rb and energy-level diagram showing all 12 transitions both ^{85}Rb and ^{87}Rb.

absorption signal $A_{12}(\nu)$ observed on the scope is 10's or 100's of millivolts high and exhibits a signal-to-noise (S/N) ratio of 50 or higher. The detector runs off of two nine-volt batteries to minimize noise; the power switch is **on** in the **up** position. **Please be sure to turn off the detector when done, so the batteries do not get drained.**

V.2.3. Getting data from the scope

The oscilloscope you use in this experiment is an Agilent digital scope, with a floppy drive. You can store your data on a floppy, say in CSV (Comma-Separated-Values) format which can easily be imported into matlab for analysis. For this experiment, you may also want to have the scope average the signal, to reduce the noise. The scope is also connected directly to the local computer's COM-1 port and data may be sent directly to Matlab or another analysis program on Athena.

VI. ANALYSIS

An exploded version of trace 3 in Figure 5 appears in Figure 6. The lineshape shows nine transitions identified as "a" through "i" in the energy-level diagram. Features a, c, d, g, and i are normal $\Delta F = \pm 1, 0$ transitions, while features b, e, f, and h are "cross-over" resonances peculiar to saturated absorption spectroscopy. To determine the hfs splitting in the $5^2S_{1/2}$ ground state of ^{87}Rb, we use transition pairs (a,g), (b,h), and (c,i) because the transitions in each of these pairs terminate on a common upper level. Hence the frequency differences $\nu_{ag} = \nu_a - \nu_g, \Delta_{bh}$, and Δ_{ci} provide direct, redundant measures of the ground state hfs. The accepted value of this splitting is $\delta\nu\left(5^2S_{1/2},^{87}Rb\right) = 6834.682614(3)$ MHz according to Penselin et al. [Phys. Rev. 127, 524 (1962)].

To complete the determination of the ground state hfs, consider the panoramic scan in Figure 7. Included is a transmission interferogram that was produced with a 48.000 cm plane-parallel Fabry-Perot cavity while the laser scanned through the spectrum.

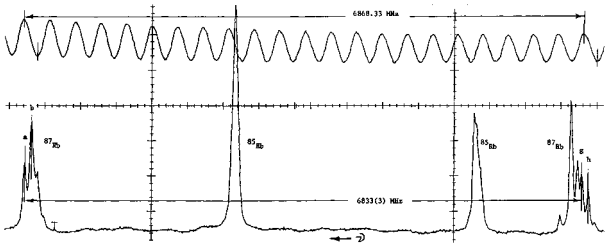

FIG. 7. Panoramic spectrum and interferogram for determination of $5^2S_{1/2}$ hfs. Please note that this particular spectrum was obtained using a research grade instrument and your own spectra may not look quite as nice.

Since the free spectral range (FSR) of this cavity is

$$\Delta\nu_{FRS} = \frac{c}{2n_{air}L} = 312.197 \text{ MHz} \tag{8}$$

it follows that every period in the interferogram corresponds to a scan increment of 312.197 MHz. To calibrate the trace in Figure 7, we use 22 periods of the interferogram corresponding to a scan range of $22(312.197) = 6868.33$ MHz and a linear distance Δx_{cal} along the chart. The linear distance between the spectral pair (a,g) is then measured and labelled Δx_{spec} . It follows that

$$\nu_{hfs}\left(5^2S_{1/2},^{87}Rb\right) = 6868.33\frac{x_{spec}}{\Delta x_{cal}} \tag{9}$$

For this particular chart, the result is $\nu_{hfs}\left(5^2S_{1/2},^{87}Rb\right) = 6833(5)MHz$, where the uncertainty reflects somewhat optimistically the accuracy with which one can locate the peaks on the interferogram. An advantage to this type of calibration, in which one uses a length of the interferogram essentially equal to the separation between the spectral features of interest, is that effects due to nonlinearities in the scan are largely suppressed. The agreement between our 6833(6) MHz and Penselin's 6834.682614 MHz is quite satisfactory. The resulting coupling constant is $A(5^2S_{1/2},^{87}Rb) = 3416(3)MHz$.

By returning to Figure 6, you can proceed to determine the hfs splittings and coupling constants for the $5^2P_{3/2}$ state. The pair of transitions (d,g) provide the basis for a determination of the F=3 to F=2 splitting, the accepted value of which is 267.1 MHz. Similarly the transition pair (g,i) permits a determination of the

middle splitting. The smallest of the splittings cannot be determined from this spectrum. Once the experimental splittings have been determined, you should proceed to evaluate the coupling constants A and B by subtracting Eq 2 from itself as discussed above. The accepted values are $A(5^2P_{3/2},^{87}Rb) = 84.85MHz$ and $B(5^2P_{3/2},^{87}Rb) = 12.51MHz$.

VI.1. Further Explorations

Once the basics of this experiment are understood, there are many avenues and variations to explore. The present version of the experiment uses laser beams that are horizontally polarized. Other polarizations are possible and the resulting effects on the lineshapes are interesting. You should experiment with different beam intensities to appreciate the tradeoff between signal strength and signal width. You should also think carefully about the nonlinearity of the laser scan and devise a method for measuring it. You might attempt also to identify the origin of the cross-over resonances and understand why they are so strong. In fluorescence spectroscopy, transition "d" would be much stronger than all the others. Why is it so weak here, and why is substantial laser power required in order to observe it?

VI.2. Suggested Theoretical Topics

1. Derive Equation 1
2. Derive Equation 2

ACKNOWLEDGEMENTS This experiment and lab guide was designed by Prof. John Brandenberger, of Lawrence University who was a visiting Professor at MIT during the 1995-96 academic year. Several other students have made valuable contributions to the development of this experiment. They are John Heanue, Gregory Richardson, Victoria Carlton, Peter Yesley and Adam Brailove.

[1] M. S. Feld and V. S. Letokhov, Sci. Am. **229**, 69 (1973), dewey Library Basement.
[2] V. S. Letokhov and V. P. Chebotayev, in *Springer Series in Optical Sciences, Vol. 4* (Springer-Verlag, New York, 1977) pp. 1–35, qC454.L3.L46 Physics Department Reading Room.
[3] V. S. Letokhov, in *High Resolution Laser Spectroscopy*, edited by K. Shimoda (Springer-Verlag, New York, 1976) Chap. 4, topics in Applied Physics, Vol. 13.
[4] P. G. P. et al., Phys. Rev. **21A**, 1955 (1980), qC.P579 Physics Department Reading Room and E-Journal.
[5] J. C. Camparo, Contemp. Phys. **27**, 443 (1985), qC.761 E-Journal.
[6] J. R. Brandenberger, Phys. Rev. **39A**, 64 (1989), qC.P579 Physics Department Reading Room and E-Journal.
[7] C. Wieman and L. Hollberg, Rev. Sci. Instrum. **62**, 1 (1991), qC.R453 Physics Department Reading Room and E-Journal.
[8] K. B. MacAdam, A. Steinbach, and C. Wieman, Am. J. Phys. **60**, 1098 (1992), qC.A513 Physics Department Reading Room and E-Journal.
[9] J. Neukammer, Optics. Comm **38**, 361 (1981).
[10] C. G. Aminoff and M. Pinard, J. Physique **43**, 273 (1982), science Library Journal Collection.
[11] S. Nakayama, J. Phys. Soc. Jap. **53**, 3351 (1984), qC.P582 Science Library Journal Collection.
[12] S. Nakayama, Jap. J. Appl. Phys. **23**, 879 (1984).
[13] G. Woodgate, "Elementary atomic structure," (Oxford University Press, 1980) Chap. 9: Hyoerfine Structure and Isotopic Shift, pp. 168–187.

8.13-14 Experimental Physics I & II "Junior Lab"

Fall 2016 - Spring 2017